International Journal of Microwave and Wireless Technologies

cambridge.org/mrf

Separately-designable diplexer with multiple transmission zeroes using common stub-loaded SIR

Yu-Jing Zhang[1], Jing Cai[2] and Jian-Xin Chen[1]

[1]School of Electronics and Information, Nantong University, 9 Seyuan road, Nantong 226019, China and [2]Affiliated Hospital of Nantong University, Nantong University, Nantong 226001, China

Research Paper

Cite this article: Zhang Y-J, Cai J, Chen J-X (2021). Separately-designable diplexer with multiple transmission zeroes using common stub-loaded SIR. *International Journal of Microwave and Wireless Technologies* **13**, 39–45. https://doi.org/10.1017/S1759078720000483

Received: 22 October 2019
Revised: 10 April 2020
Accepted: 14 April 2020
First published online: 15 May 2020

Key words:
Diplexer; separately-designable; stub-loaded SIR; transmission zero (TZ)

Author for correspondence:
Jing Cai, E-mail: caijing2005@163.com

Abstract

A separately-designable diplexer with multiple transmission zeroes (TZs) using common stub-loaded stepped impedance resonator (SIR) is proposed. The common stub-loaded SIR operating in third harmonic (f_3) and fifth harmonic (f_5) is used for designing the two diplexer channels. The stub is loaded at the voltage-null point of f_3 of the SIR. It can separately control f_5 but has no effect on f_3 so that the two channels can be separately designed. Meanwhile, the input port is tap-connected to the common stub-loaded SIR, which necessarily produces a TZ between f_3 and f_5, existing in both channel filtering responses. By properly choosing coupling schemes of the two channels, more TZs are realized at the desired locations. Thanks to the generation of the multiple TZs, both passband selectivity and isolation between the two channels are improved significantly. For demonstration, a diplexer operating at 2.22 and 2.95 GHz is designed, fabricated, and measured. The simulated and measured results are presented, showing good agreement.

Introduction

Diplexers/multiplexers are important components in wireless communication systems that can separate the signals from the same input port to two or more different channels according to their own frequencies. With the stringent requirements in modern communication systems, it is demanded that they have small size, low loss, high isolation, flexible channel frequencies, and so on. Therefore, various kinds of diplexers/multiplexers have been developed for modern transceivers, such as substrate integrated waveguide (SIW) [1–3], cavity [4–7], slotline [8, 9], coplanar waveguide structure [10], and microstrip [11–24].

In order to avoid employing the combining network and reduce the size, the adoption of common resonator at the input is a good solution, and it acts as a *T*-junction and the first resonator for both channels. In [1], the common dual-mode (TE_{101} and TE_{201}) cavity is applied for designing SIW diplexer, while the frequencies and channel responses are difficult to be separately designed. Moreover, the large size of SIW makes it unsuitable for miniaturized systems. To reduce the size, the common T-shaped resonator in [15, 16] is used to design microstrip diplexers. But the channel frequencies and responses cannot be flexibly designed yet, which inevitably increases the design complexity. Recently, a centrally-loaded half wavelength ($\lambda/2$) uniform-impedance resonator (UIR) is developed for the input common resonator, and with the aid of loaded stub, the two channel filters can be separately designed. However, all employed resonators are $\lambda/2$ ones. They have to be folded in many times and distribute in many layers in the low-temperature co-fired ceramic, which reduces the unloaded quality factor (Q_u) of the resonator and then increases the passband loss.

In this letter, a common stub-loaded stepped impedance resonator (SIR) is investigated and used as a common input resonator to design a diplexer with multiple transmission zeroes (TZs). The stub is loaded at the voltage-null point of third harmonic f_3 of the SIR. It can separately control fifth harmonic f_5 but has no effect on f_3 so that the two channels of the diplexer can be separately designed. The input feed position on the stub-loaded SIR can be properly designed to generate a common TZ between f_5 and f_3, which exists in both channel filtering responses. Meanwhile, the coupling schemes of two channels can generate a TZ at the passband frequency of the other channel filter. Due to the existing of multiple TZs, the selectivity and isolation of the proposed diplexer can be improved significantly.

Stub-loaded SIR

Figure 1(a) shows the configuration of the SIR, where Z_i and l_i ($i = 1$ or 2) are the characteristic impedance and physical length of the transmission line, respectively. Figure 1(b) plots f_5/f_3 against u under different R_Z, where $R_Z = Z_1/Z_2$ and $u = l_1/(l_1 + l_2)$. The zoomed illustration

© Cambridge University Press and the European Microwave Association 2020

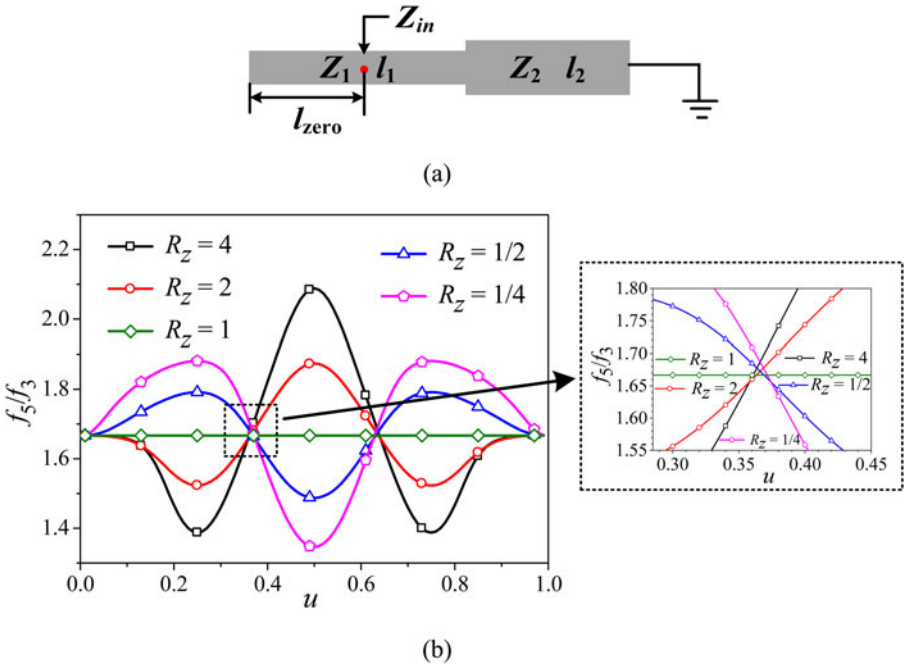


Fig. 1. (a) Traditional $\lambda/4$ SIR, (b) f_5/f_3 against u under different R_Z and its zoomed illustration.

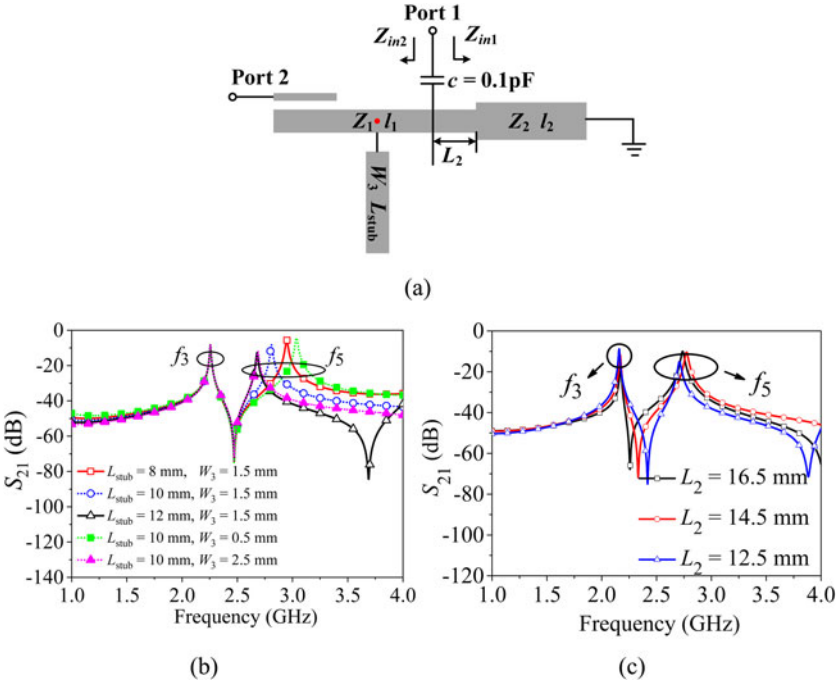


Fig. 2. (a) A weak coupling structure for analyzing the stub-loaded SIR, (b) frequency response against different stub length L_{stub} and W_3 when $L_2 = 14.5$ mm and (c) different L_2 when $L_{stub} = 10$ mm and $W_3 = 1.5$ mm.

clearly shows the confluence of five curves. In this design, f_5 and f_3 are chosen for the two channels and they can be close to each other. Accordingly, $R_Z = 2.3$ and $u = 2/3$ are selected. Once the total physical length is given, both f_5 and f_3 can be calculated. Meanwhile, the voltage-null point (red point in Fig. 1) of f_3 should be located on the section with Z_1 of the SIR and can be determined by (1) below [25], where $\mathrm{Im}[Z_{\mathrm{in}}] = 0$

$$\tan(\beta l_2) + R_z \tan(\beta l_1 - \beta l_1 u_R) = 0. \quad (1)$$

Substituting $R_Z = 2.3$ and $u = 2/3$ into (1), $u_R = l_0/(l_1 + l_2) = 0.33$ can be obtained.

To achieve the separate design of f_5 and f_3, a stub is attached to the voltage-null point of f_3 on the SIR, as shown in Fig. 2(a). It can be seen from Fig. 2(b) that as L_{stub} or W_3 increases, f_5 shifts down and is gradually close to f_3 (fixed) so that the two close channels of the diplexer can be easily achieved. It can also be found that there is a TZ between f_3 and f_5, which depends on the location of feeding point (represented by L_2), as shown in Fig. 2(c). According to the transmission line theory, the input impedance

https://doi.org/10.1017/S1759078720000483 Published online by Cambridge University Press

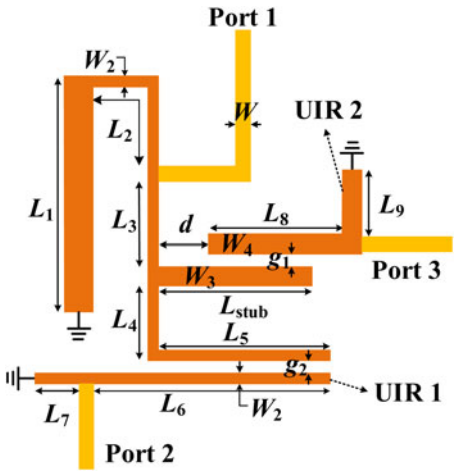


Fig. 3. Layout of the proposed diplexer.

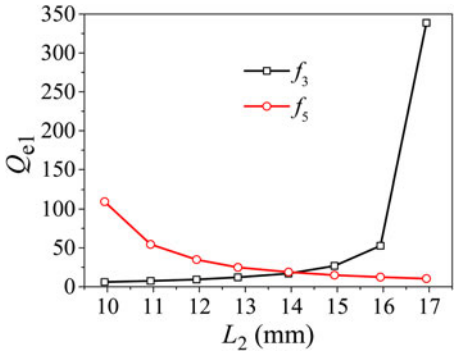


Fig. 4. The Q_e of Port 1 versus L_2 at the frequency of f_3 and f_5.

Z_{int} at the input port 1 can be expressed as

$$Z_{int} = \frac{Z_{in1}Z_{in2}}{Z_{in1} + Z_{in2}}. \quad (2)$$

Since the feeding point is at the right of the voltage-null point of f_3, the frequency f_{TZ} of the TZ corresponding to $Z_{int} = 0$ (due to $Z_{in1} = 0$) is larger than f_3. Similar to f_3, when the feeding point is located at the left of the voltage-null point of f_5, the f_{TZ} can be smaller than f_5. As can be seen from Fig. 2(c), f_{TZ} moves from f_3 to f_5 when L_2 increases. It is worthy to note that the TZ simultaneously exists in both channels so that the passband selectivity and isolation between the two channels can be enhanced greatly in the following design of diplexer.

Design of the proposed diplexer

Figure 3 shows the layout of the proposed diplexer. Port 1 is tap-connected to the common stub-loaded SIR operating at f_3 and f_5 for the lower and higher channels, respectively. The tapped position of Port 1 not only determines the location of the common TZ, but also affects the input external quality factor (Q_e) of Port 1. A $\lambda/4$ UIR tapped by Port 2 (UIR1) couples with a part of common SIR to form the lower channel. The stub loaded at the voltage-null point of f_3 on the SIR is coupled with another $\lambda/4$ UIR tapped by Port 3 (UIR2) to construct the higher channel. In this design, the parameters of the UIRs can be optimized to achieve the desired Q_es for both channels. Benefiting from the loading scheme of the common SIR, the stub can separately control f_5 but has no effect on f_3. As a result, the two channels of the proposed diplexer can be separately designed (as shown in Figs 5(a) and 7(a)) so that the respective specifications of the channels can be easily realized.

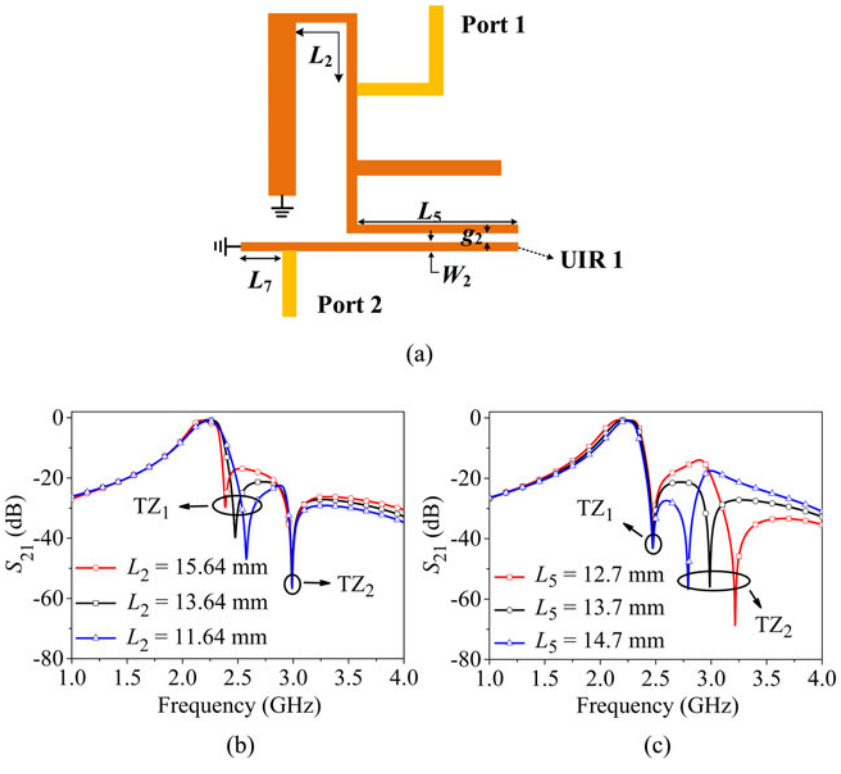


Fig. 5. (a) The structure of lower channel, (b) TZ_1 changes with different length L_2 when $L_5 = 13.7$ mm, $L_7 = 16.4$ mm, $W_2 = 0.5$ mm, and $g_2 = 0.1$ mm, (c) TZ_2 changes with different length L_5 when $L_2 = 13.64$ mm, $L_7 = 16.4$ mm, $W_2 = 0.5$ mm, and $g_2 = 0.1$ mm.

https://doi.org/10.1017/S1759078720000483 Published online by Cambridge University Press

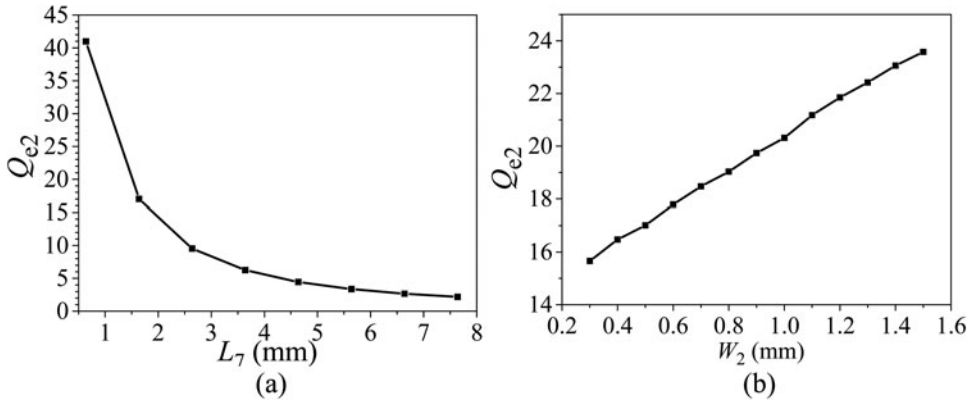


Fig. 6. The Q_e of Port 2 versus different (a) L_7 when $W_2 = 0.5$ mm, (b) W_2 when $L_7 = 1.64$ mm.

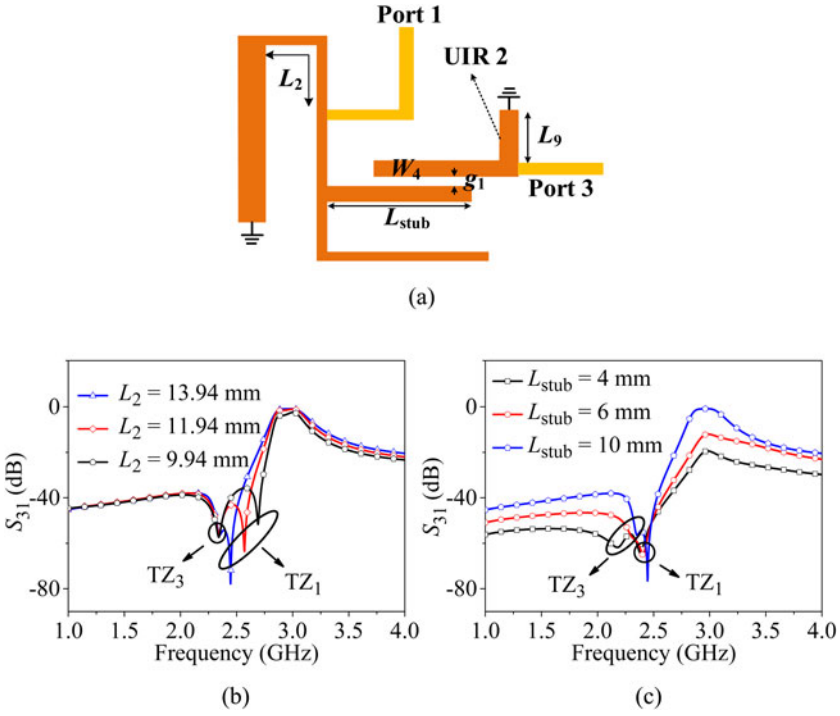


Fig. 7. (a) The structure of higher channel, (b) TZ_1 changes with different length L_2 when $L_{stub} = 6$ mm, $W_4 = 1.5$ mm, and $g_1 = 0.4$ mm, (c) TZ_3 changes with different length L_{stub} when $L_2 = 11.94$ mm, $W_4 = 1.5$ mm, and $g_1 = 0.4$ mm.

Design of Q_e at the common port (Port 1)

Due to the simultaneous impact of Q_e and TZ by the tapped position of Port 1, the variation of input Q_e (Q_{e1}) should be studied. When the Q_{e1} is fixed, the Q_es of the other two ports (Q_{e2} for Port 2 and Q_{e3} for Port 3) should meet the desired Q_e, which is the value of Q_{e1}. Hence, the Q_es of the three ports should be extracted.

The Q_e can be extracted and attained by

$$Q_e = \frac{f_0}{f_{\pm 90^\circ}}, \tag{3}$$

where f_0 and $f_{\pm 90^\circ}$ denote the central frequency and the ±90° bandwidth with respect to the absolute phase at f_0, respectively. The extracting procedures are as follow:

(1) Set the capacitor $c = 0.1$ pF to realize a weak coupling between feedline and resonator as shown in Fig. 2(a).
(2) Simulate the structure to obtain the phases in different f_0.
(3) Calculate the ±90° bandwidth of absolute phase at different f_0.
(4) Calculate Q_es at different frequencies by using Eq. (3).

The Q_{e1} under different L_2 is extracted and shown in Fig. 4. As can be seen, the variation trend of Q_{e1} is different when the frequency changes. In this paper, the $L_2 = 13.94$ mm is chosen for the equivalent $Q_{e1} = 17$ at f_3 and f_5. Hence, the equivalent fractional bandwidth (about 9%) of both channels can be achieved, which would be popular in practical applications.

Design of the lower channel

For the lower channel filter operating in f_3 of the common SIR, the $\lambda/4$ UIR tapped by Port 3 coupled with the stub can be

https://doi.org/10.1017/S1759078720000483 Published online by Cambridge University Press

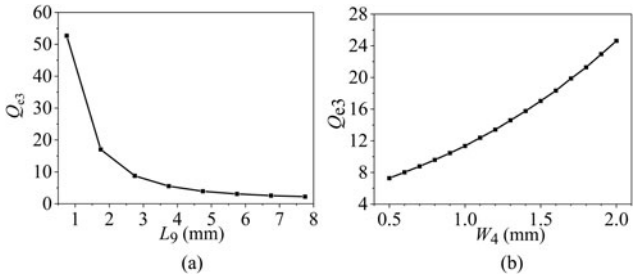


Fig. 8. The Q_e of Port 3 versus different (a) L_9 when $W_4 = 1.5$ mm, (b) W_4 when $L_9 = 1.75$ mm.

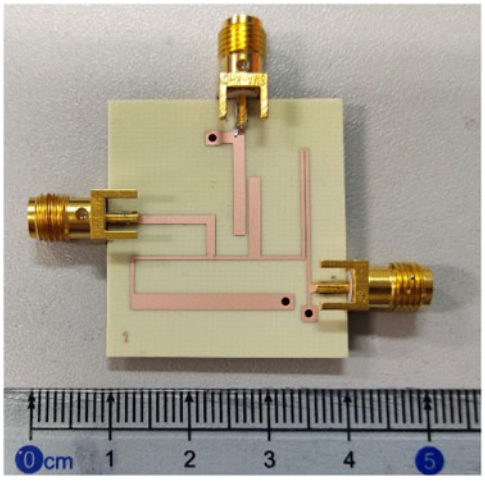


Fig. 9. The photograph of the fabricated diplexer.

removed, as shown in Fig. 5(a). This is because the loaded stub has no effect on f_3 and can be ignored here. As expected, a TZ (TZ_1 shown in Figs 5(b) and 5(c)) is obtained, resulting from the tapped feeding scheme of the common SIR. To achieve high isolation, another TZ (TZ_2) is designed by using the parallel coupling structure with length L_5, which corresponds to the $\lambda/4$ at the frequency of TZ_2. The TZ_2 can be easily tuned by tuning L_5 and located in the upper channel, as shown in Fig. 5(c). Once L_5 is determined, the coupling coefficient between the SIR and UIR1 (K_{12}) can be controlled by the coupling gap g_2.

For constructing the lower channel, the Q_{e2} should be equaled to the desired Q_{e1} at the frequency of f_3. The Q_{e2} are extracted and

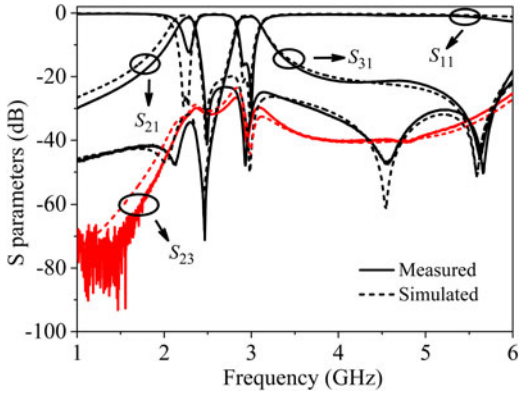


Fig. 10. Simulated and measured results of the proposed diplexer.

shown in Fig. 6. As can be seen, the tapped position of Port 2 (L_7) and the width of UIR1 (W_2) can be optimized to meet the desired Q_e. As the desired Q_e is obtained in Port 2, the desired K_{12}, which meets the requirement of 9% 3 dB fractional bandwidth, can be obtained by easily changing g_2. Until now, the lower channel has been constructed.

Design of the higher channel

For the higher channel filter operating in f_5 of the common SIR, another $\lambda/4$ UIR tapped by Port 3 (UIR2) is used to couple with the stub. Since the loaded stub on the common SIR has no effect on f_3, it can be used to control the higher channel frequency alone. In this design, the UIR1 can also be removed, as shown in Fig. 7(a), because the coupling structure with length L_5 in the lower channel path can be regarded as an open circuit at f_5, indicated by TZ_2 in Fig. 5. Similar to the lower channel filter, a TZ (TZ_1 shown in Figs. 7(b) and 7(c)) is obtained, resulting from the tapped feeding scheme of the common SIR. To achieve high isolation, an extra TZ (TZ_3) in the lower stopband can be generated, as shown in Fig. 7(c), and it can be optimized by tuning stub length L_{stub} as well as the coupling length between the stub and UIR2 to be located in the lower channel.

Similar to the design of Q_{e2}, the desired Q_e can be also obtained by optimizing the tapped position of Port 3 (L_9) and the width of the UIR2 (W_4) for constructing the higher channel, as shown in Fig. 8. When the desired Q_e is obtained in Port 3, the desired coupling coefficient between the SIR and UIR2 (K_{13}) can be obtained by easily changing g_1.

Table 1. Performance comparison with other previous diplexers

Ref.	Order	f_L/f_H (GHz)	IL (dB)	Separately-designable	Isolation (dB)	Size ($\lambda_g \times \lambda_g$)	Fabrication technology
[1]	3	12/14	1.34/1.41	No	>27	1.99 × 1.39	SIW
[15]	2	1.95/2.14	1.46/1.44	No	>36	0.38 × 0.56	Microstrip
[16]	3	1.95/2.14	1.2/1.5	No	>35	0.36 × 0.38	Microstrip
[18]	2	3.55/5.55	1.74/2.37	Yes	>40	0.054 × 0.048	LTCC
[19]	2	2.41/3.61	1.46/2.15	No	>38	0.66 × 0.15	Microstrip
[26]	2	1.82/2.41	2.2/2.1	No	>30	0.19 × 0.34	Microstrip
[27]	2	1.84/2.42	N/A	No	>30	0.64 × 0.59	Microstrip
This work	2	2.22/2.95	1.14/1.42	Yes	>30	0.32 × 0.34	Microstrip

https://doi.org/10.1017/S1759078720000483 Published online by Cambridge University Press

The specific design procedures are as follows:

(1) According to the transmission line theory, the original frequency of f_3 and f_5 can be designed by choosing the appropriate length and R_z of the SIR. The f_5 can be altered to the desired frequency by changing the length and width of the loaded-stub (L_{stub} and W_3);
(2) In order to produce a TZ between f_3 and f_5, the input line is tap-connected to the SIR as the feed point is loaded between the voltage-null point of f_3 and f_5. The TZ can be controlled by the location of the feed point;
(3) A $\lambda/4$ UIR is coupled to the open-end of the SIR to build the lower channel of the diplexer (at the frequency of f_3). An extra TZ (TZ_2) can be generated and altered by the coupling length L_5. The desired Q_e and K_{12} can be obtained by the tapped-location of Port 2 (L_7), the width of the UIR1 (W_2), and the coupling gap (g_2).
(4) Similar to the design of the lower channel, another $\lambda/4$ UIR is coupled to the stub to build the higher channel of the diplexer (at the frequency of f_5). An extra TZ (TZ_3) can be generated and altered by the L_{stub}. The desired Q_e and K_{13} can be obtained by the tapped-location of Port 3 (L_9), the width of the UIR2 (W_4), and the coupling gap (g_1).

Based on the above analysis, the diplexer can be designed by combining the lower and higher channel filters, as shown in Fig. 3. By properly choosing the two coupled schemes and the feed position of the input port, each channel filter can generate two TZs in the vicinity of the other channel filter frequency, resulting in high selectivity and high isolation.

Simulated and measured results

The simulation and experiment of the proposed diplexer are conducted by using Ansoft HFSS and Agilent N5230A network analyzer, which can measure the mixed *S* parameters directly. Rogers RO4003c substrate with a dielectric constant of 3.38 and a thickness of 0.508 mm is used in this design. The structure parameters for the proposed diplexer are $L_1 = 20$ mm, $L_2 = 13.94$ mm, $L_3 = 4.19$ mm, $L_4 = 5.55$ mm, $L_5 = 13.7$ mm, $L_6 = 17.24$ mm, $L_7 = 1.64$ mm, $L_8 = 11.84$ mm, $L_9 = 1.75$ mm, $L_{stub} = 10$ mm, $W = 1.122$ mm, $W_1 = 2$ mm, $W_2 = 0.5$ mm, $W_3 = 1.5$ mm, $W_4 = 1.5$ mm, $d = 2.5$ mm, $g_1 = 0.4$ mm, and $g_2 = 0.1$ mm. The photograph of the fabricated diplexer is shown in Fig. 9. Figure 10 shows the simulated and measured *S* parameter results of the proposed diplexer. The measured two passbands are centered at 2.28 and 2.95 GHz with the 3 dB fractional bandwidth of 8.9 and 9.3%. The insertion losses are 1.45 and 1.15 dB at the two center frequencies and the return losses in the two passbands are better than 12 dB. The common TZ_1 between two channels is located at 2.46 GHz. The TZ_2 and TZ_3 in the lower and higher channel are located at 2.95 and 2.1 GHz, respectively, and then the isolations within the two passbands are better than 30 and 40 dB. The bandwidth of the lower channel in the measured result is smaller than that in the simulated result as shown in Fig. 10. That is because the coupling gap between the SIR and UIR1 ($g_2 = 0.1$ mm) is too small to guarantee the fabricated accuracy.

Table 1 summarizes the performance comparison between the proposed design and the reported diplexer. It can be found that the proposed diplexer has low loss and simple design procedure due to the separate controlling of two bandpass response.

Conclusion

In this paper, a separately-designable diplexer with multiple TZs using a common stub-loaded SIR has been presented. Based on the stub-loaded stub and proper coupling scheme, the two channels can be separately designed, showing a simplified design method. Several TZs are generated to improve the selectivity and isolation. The proposed diplexer has been validated by the simulation and experiment. It owns several advantages such as low loss, good selectivity, and isolation, which would be a good candidate for many practical applications.

Acknowledgment. This work was supported by the Science-Technology Programs of Nantong, China (Grant No. MS12018004).

References

1. **Zhou K, Zhou CX and Wu W** (2018) Compact SIW diplexer with flexibly allocated bandwidths using common dual-mode cavities. *IEEE Microwave and Wireless Components Letters* **28**, 317–319.
2. **Dong Y and Itoh T** (2011) Substrate integrated waveguide loaded by complementary split-ring resonators for miniaturized diplexer design. *IEEE Microwave and Wireless Components Letters* **21**, 10–12.
3. **Song KJ, Zhou Y, Chen YX, Iman AM, Patience SR and Fan Y** (2019) High-isolation diplexer with high frequency selectivity using substrate integrate waveguide dual-mode resonator. *IEEE Access* **7**, 116676–116683.
4. **Nocella V, Pelliccia L, Farinelli P, Sorrentino R, Costa M, Yufeng D and Yanzhao Z** (2016) E-band cavity diplexer based on micromachined technology. *International Journal of Microwave and Wireless Technologies* **8**, 179–184.
5. **Wong SW, Li JY, Yang Y, Zhu H, Chen RS, Zhu L and He YJ** (2020) Cavity balanced and unbalanced diplexer based on triple-mode resonator. *IEEE Transactions on Industrial Electronics* **67**, 4969–4979.
6. **Ezzeddine H, Bila S, Verdeyme S, Seyfert F, Pacaud D, Puech J and Estagerie L** (2012) Compact diplexers and triplexers implemented with dual-mode cavities. *International Journal of Microwave and Wireless Technologies* **4**, 51–58.
7. **Qi ZH, Li XP and Zeng JJ** (2018) Wideband diplexer design and optimization based on back-to-back structured common port. *IEEE Microwave and Wireless Components Letters* **28**, 320–322.
8. **Liu HW, Xu WY, Zhang ZC and Guan XH** (2013) Compact diplexer using slotline stepped impedance resonator. *IEEE Microwave and Wireless Components Letters* **23**, 75–77.
9. **Chen D, Zhu L, Bu H and Cheng C** (2015) A novel planar diplexer using slotline-loaded microstrip ring resonator. *IEEE Microwave and Wireless Components Letters* **25**, 706–708.
10. **Zheng T, Wei B, Gao B, Guo XB, Zhang XP, Jiang LA, Xu Z and Heng Y** (2015) Compact superconducting diplexer design with conductor-backed coplanar waveguide structures. *IEEE Transactions on Applied Superconductivity* **25**, 1–4.
11. **Rezaei A and Noori L** (2018) Novel compact microstrip diplexer for GSM applications. *International Journal of Microwave and Wireless Technologies* **10**, 313–317.
12. **Peng HS and Chiang YC** (2015) Microstrip diplexer constructed with new types of dual-mode ring filters. *IEEE Microwave and Wireless Components Letters* **25**, 7–9.
13. **Noori L and Rezaei A** (2017) Design of a microstrip dual-frequency diplexer using microstrip cells analysis and coupled lines components. *International Journal of Microwave and Wireless Technologies* **9**, 1467–1471.
14. **Tizyi H, Riouch F, Tribak A, Najid A and Mediavilla A** (2018) Microstrip diplexer design based on two square open loop bandpass filters for RFID applications. *International Journal of Microwave and Wireless Technologies* **10**, 412–421.
15. **Chuang ML and Wu MT** (2011) Microstrip diplexer design using common T-shaped resonator. *IEEE Microwave and Wireless Components Letters* **21**, 583–585.

https://doi.org/10.1017/S1759078720000483 Published online by Cambridge University Press

16. **Guan XH, Yang FQ, Liu HW and Zhu L** (2104) Compact and high-isolation diplexer using dual-mode stub-loaded resonators. *IEEE Microwave and Wireless Components Letters* **24**, 385–387.
17. **Xu J, Chen ZY and Zhu YX** (2019) Dual-plane quadruplexer using common lumped-element quadruple-mode resonator. *IEEE Microwave and Wireless Components Letters* **29**, 617–619.
18. **Xu JX and Zhang XY** (2017) Compact high-isolation LTCC diplexer using common stub-loaded resonator with controllable frequencies and bandwidths. *IEEE Transactions on Microwave Theory and Techniques* **65**, 4636–4644.
19. **Xiao J, Zhang M and Ma J** (2018) A compact and high-isolated multiresonator-coupled diplexer. *IEEE Microwave and Wireless Components Letters* **28**, 999–1001.
20. **Duong T, Hong W, Hao Z, Huang W, Zhuang J and Vo V** (2016) A millimeter wave high-isolation diplexer using selectivity-improved dual-mode filters. *IEEE Microwave and Wireless Components Letters* **26**, 104–106.
21. **Weng M, Hung C and Su Y** (2007) A hairpin line diplexer for direct sequence ultra-wideband wireless communications. *IEEE Microwave and Wireless Components Letters* **17**, 519–521.
22. **Yang T, Chi P and Itoh T** (2010) High isolation and compact diplexer using the hybrid resonators. *IEEE Microwave and Wireless Components Letters* **20**, 551–553.
23. **Xiao J, Zhu M, Li Y, Tian L and Ma J** (2015) High selective microstrip bandpass filter and diplexer with mixed electromagnetic coupling. *IEEE Microwave and Wireless Components Letters* **25**, 781–783.
24. **Chen C, Lin C, Tseng B and Chang S** (2014) High-isolation and high-rejection microstrip diplexer with independently controllable transmission zeros. *IEEE Microwave and Wireless Components Letters* **24**, 851–853.
25. **Li YL, Chen JX, Qin W, Lu QY and Bao ZH** (2017) Millimetre-wave low-temperature co-fired ceramic bandpass filter with independently controllable dual passbands. *IET Microwaves, Antennas & Propagation* **11**, 1558–1564.
26. **Yan J, Zhou H and Cao L** (2016) Compact diplexer using microstrip half- and quarter-wavelength resonators. *Electronics Letters* **52**, 1613–1615.
27. **Feng WJ, Gao X and Che WQ** (2014) Microstrip diplexer for GSM and WLAN bands using common shorted stubs. *Electronics Letters* **50**, 1486–1488.



Yu-Jing Zhang was born in Nantong, Jiangsu Province, China, in 1995. She received the B.Sc. Degree in electronic science and technology from Nantong University, Nantong, China, in 2017. She is currently pursuing the M.Sc. degree in electromagnetic field and microwave technology in Nantong University, Nantong, China. Her current research interests include microwave passive and reconfigurable filters.



Jing Cai was born in Nantong, Jiangsu Province, China, in 1992. He received the B.Sc. degree in biomedical engineering from Nantong University, Nantong, China, in 2015, and the M.Sc. degree in information and communication engineering from Nantong University, Nantong, China, in 2018. His current research interests include microwave passive and reconfigurable filters.



Jian-Xin Chen received the B.S. degree from Huai Yin Teachers College, Huai'an, China, in 2001, the M.S. degree from the University of Electronic Science and Technology of China (UESTC), Chengdu, China, in 2004, and the Ph.D. degree from the City University of Hong Kong, Hong Kong, in 2008. Since 2009, he has been with Nantong University, Nantong, China, where he is currently a Professor. He has authored or co-authored more than 100 academic papers. He holds 15 Chinese patents and three US patents. His research interests include RF/microwave differential circuits and antennas, dielectric resonator (DR) filters, and low-temperature co-fired ceramic circuits and antennas. Dr. Chen received the Best Paper Award presented at the Chinese National Microwave and Millimeter-Wave Symposium, Ningbo, China, in 2007. He was the Supervisor of 2014 iWEM student innovation competition winner in Sapporo, Japan.

https://doi.org/10.1017/S1759078720000483 Published online by Cambridge University Press